

Supporting Information

A pH-driven molecular shuttle based on rotaxane-bridged periodic
mesoporous organosilicas with responsive release of guests

*Meng Gao,^a Shuhua Han,^{*a} Yongfeng Hu,^b James J. Dynes,^b Xiangguo Liu^c and
Dongniu Wang^b*

^aKey Lab of Colloid and Interface Chemistry Ministry of Education , Shandong

University, Jinan 250100, P. R. China

^bCanadian Light Source 44 Innovation Boulevard Saskatoon, SK, S7N 2V3, Canada

^cDivision of Cell Biology, School of Life Sciences, Shandong University, Jinan, 250100,

P. R. China

*Corresponding Author's Contact Information: E-mail: shuhhan@sdu.edu.cn;

Tel: (+86)531-8836-5450

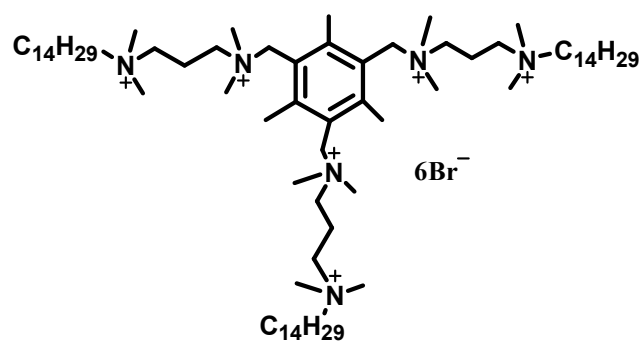


Figure S1. The chemical structure of 2, 4, 6-tris ((2-N,N-dimethyl, 6-N',N',N'-dimethyltetradecyl) hexane di-ammonium) mesitylene hex-bromide (sym-Ph(1-3-14)₃)

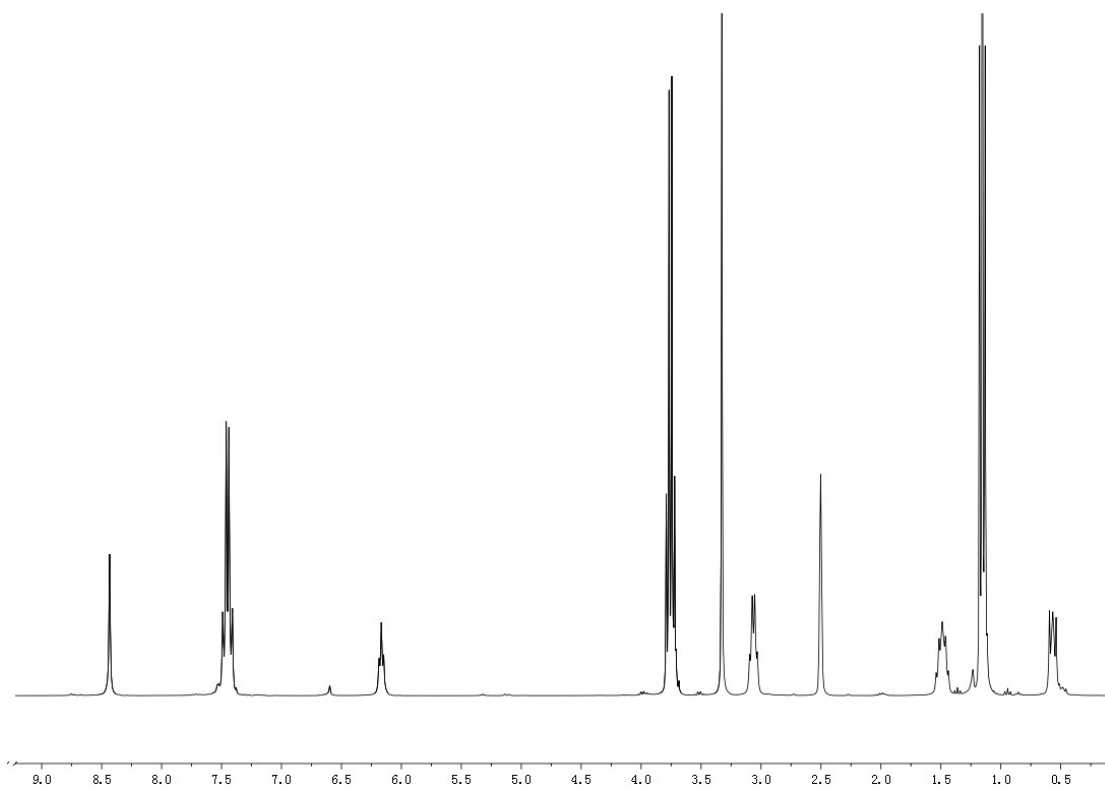


Figure S2. ^1H NMR spectra of BpU.

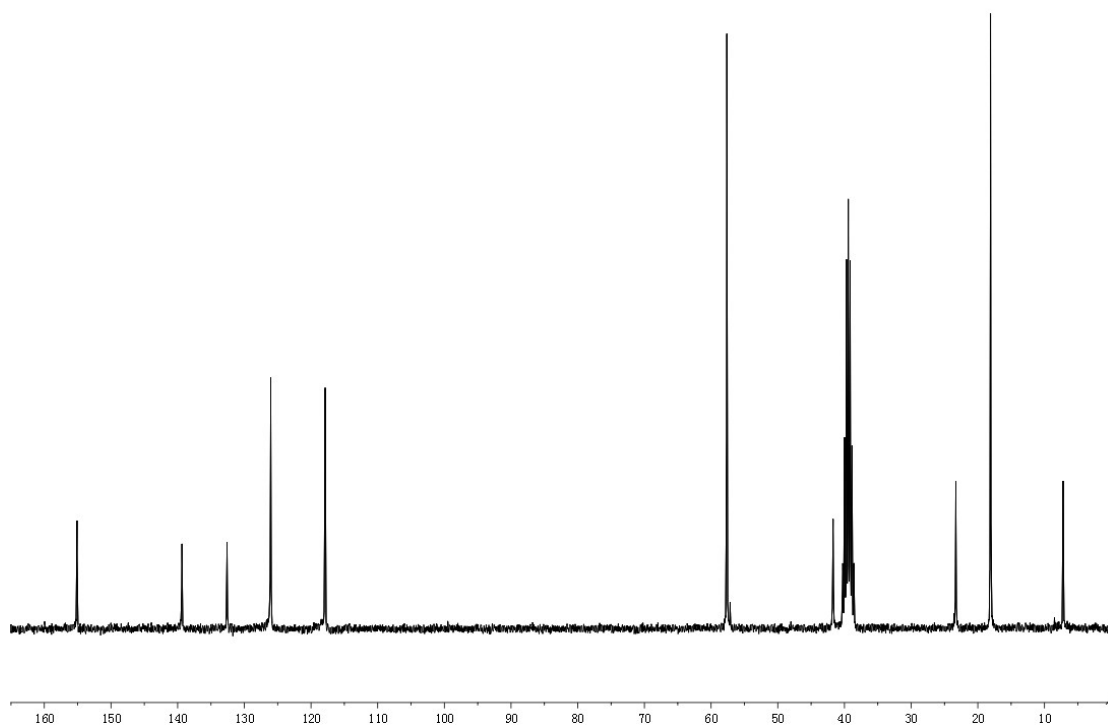


Figure S3. ^{13}C NMR spectra of BpU.

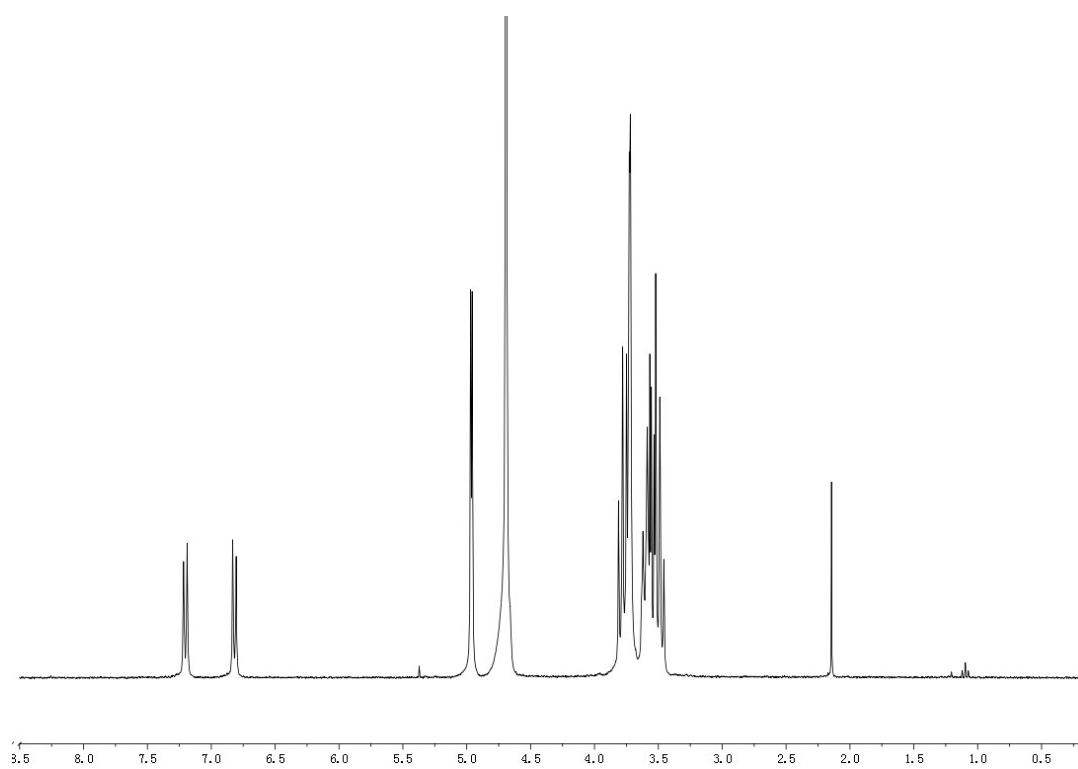


Figure S4. ^1H NMR spectra of benzidine- CD_2 .

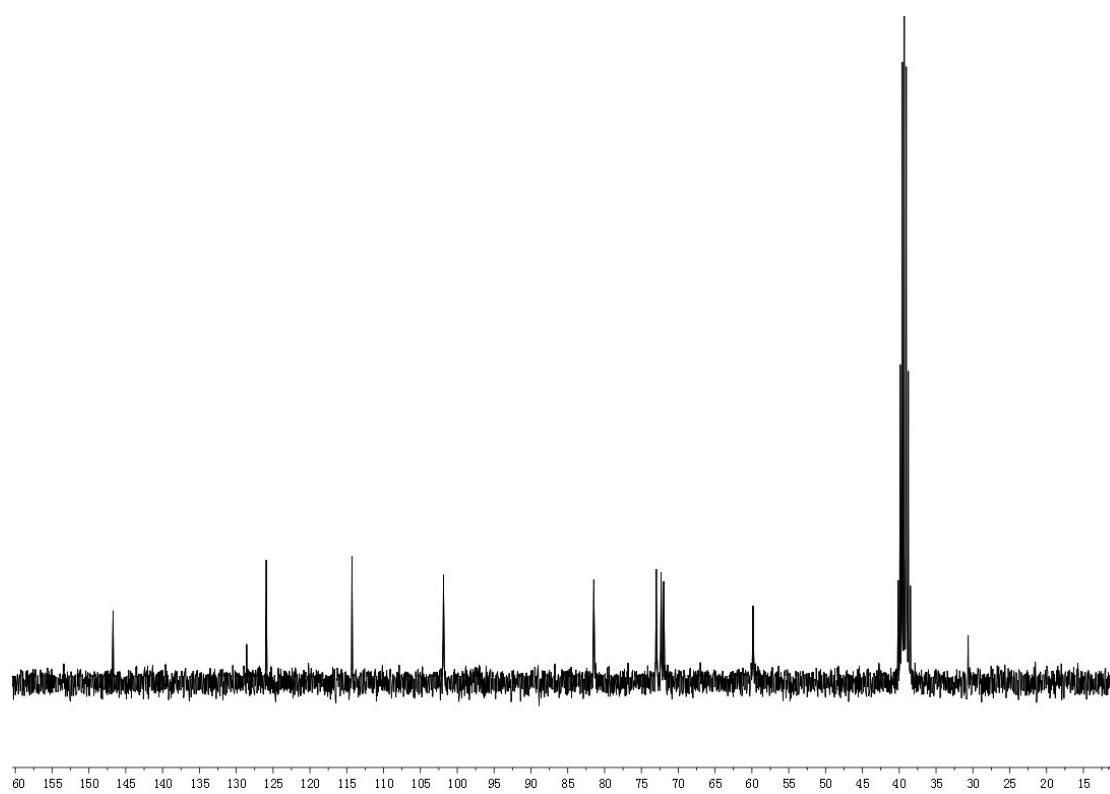


Figure S5. ^{13}C NMR spectra of benzidine- CD_2 .

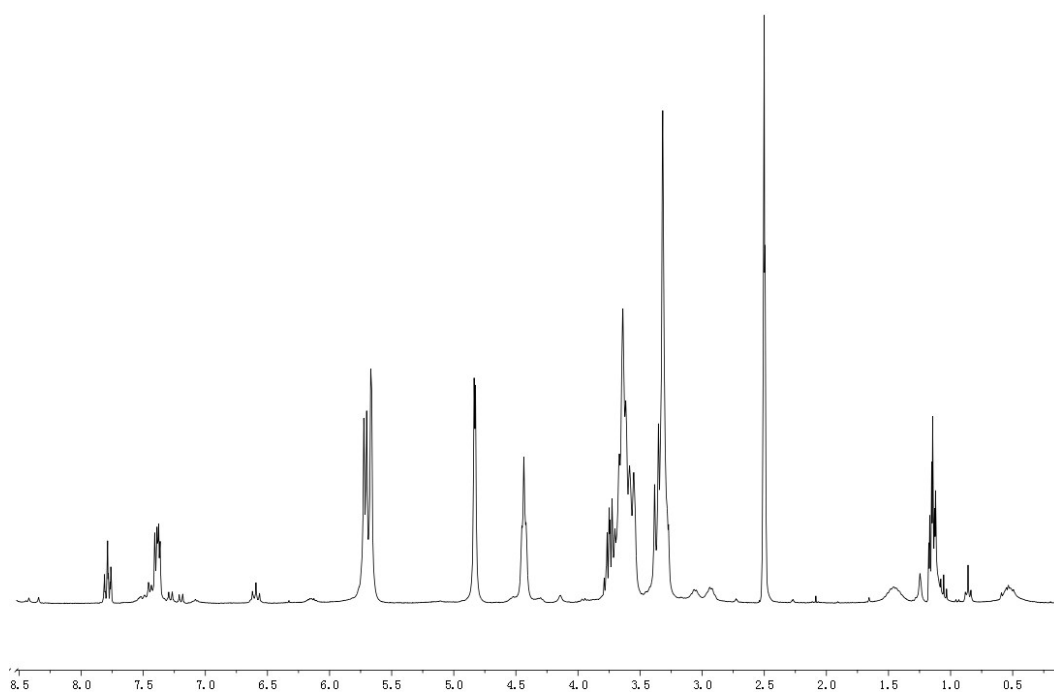


Figure S6. ^1H NMR spectrum of $\text{BpU}\text{-CD}_2$.

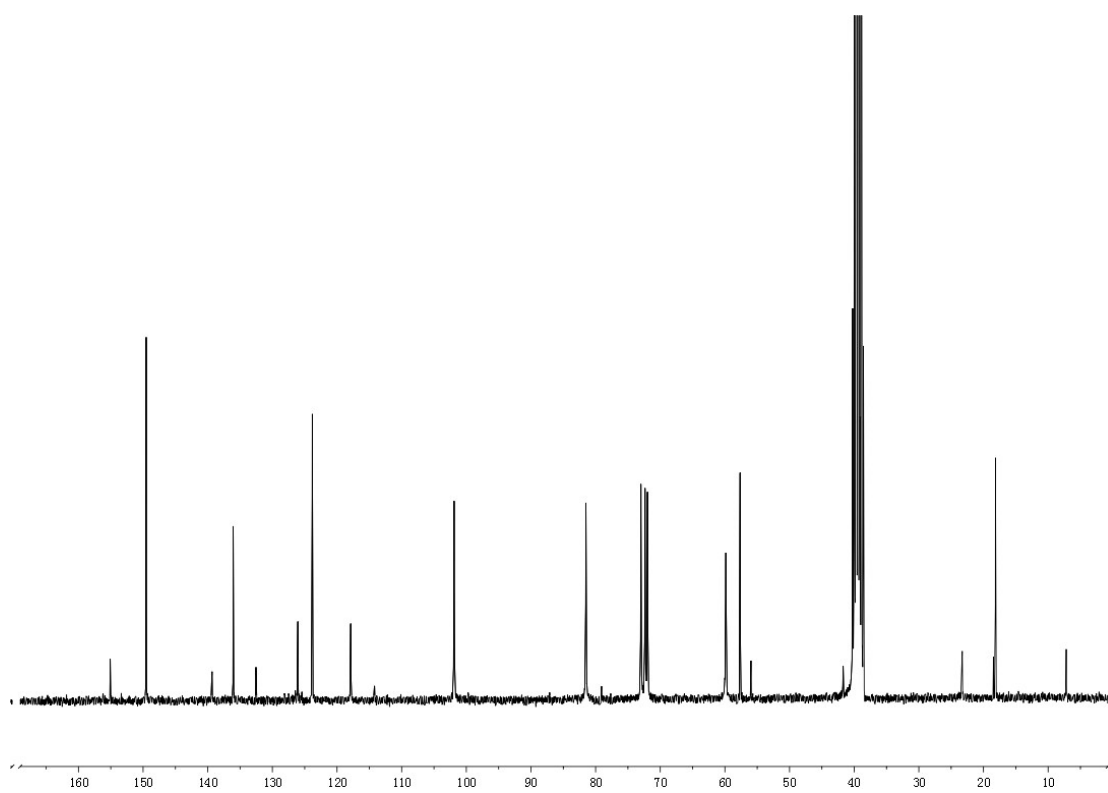


Figure S7. ^{13}C NMR spectrum of $\text{BpU}\text{-CD}_2$.

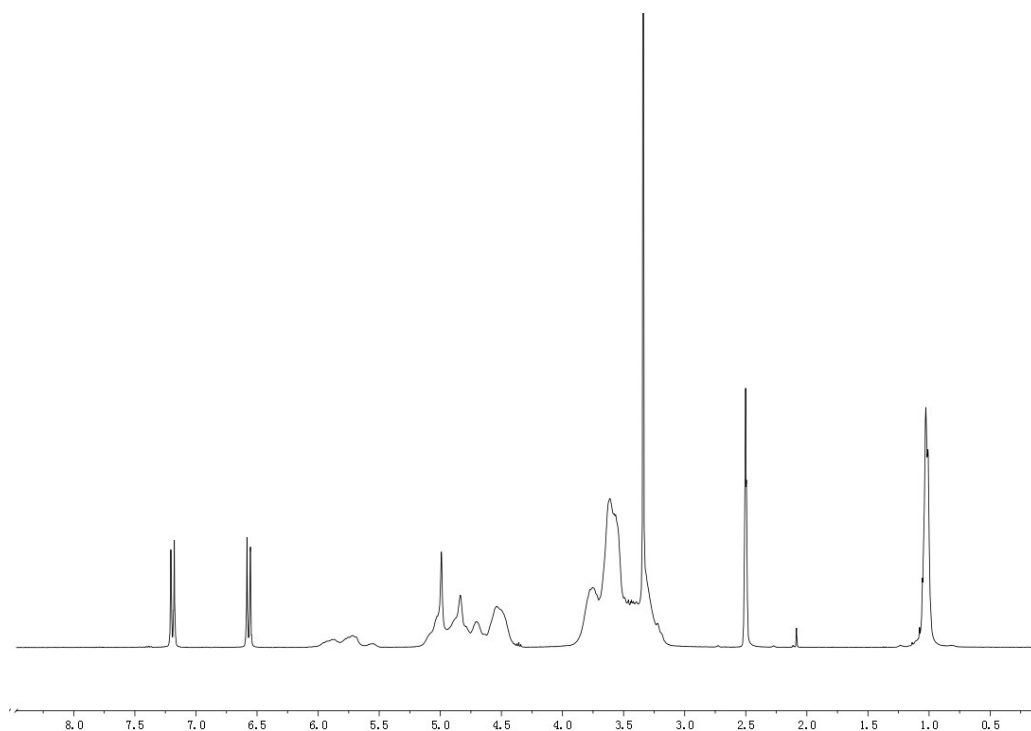


Figure S8. ^1H NMR spectrum of benzidine \subset HpCD.

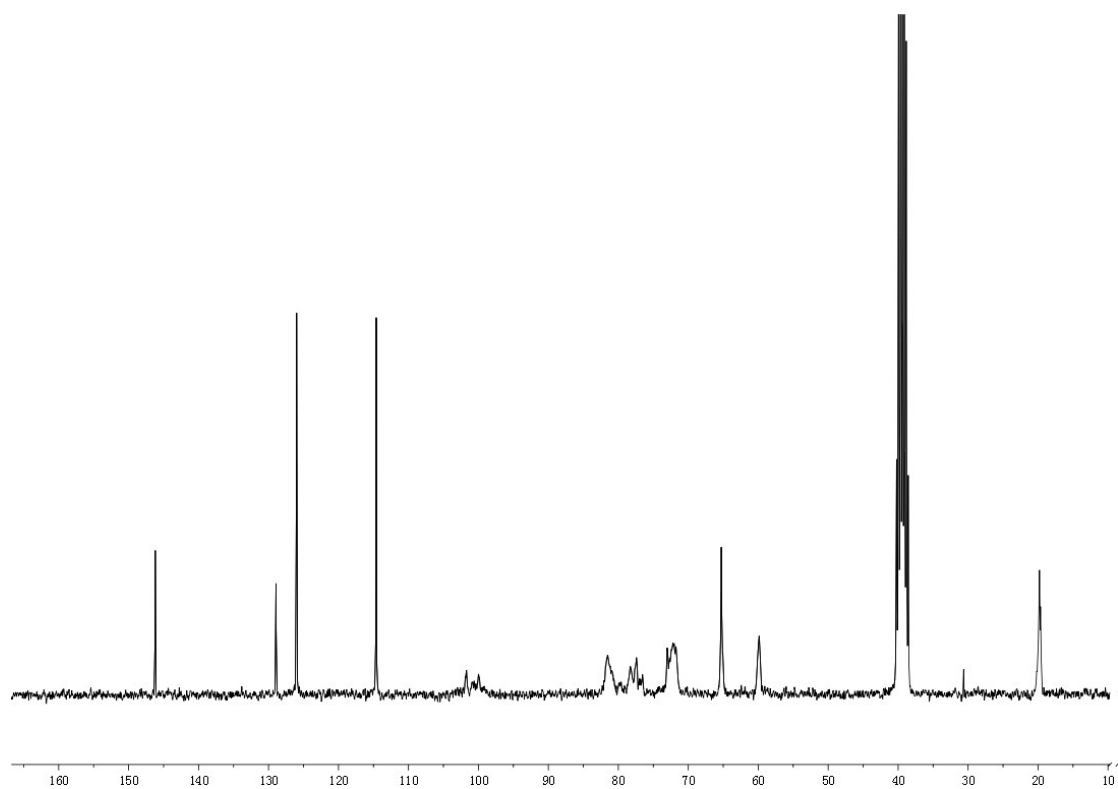


Figure S9. ^{13}C NMR spectrum of benzidine \subset HpCD.

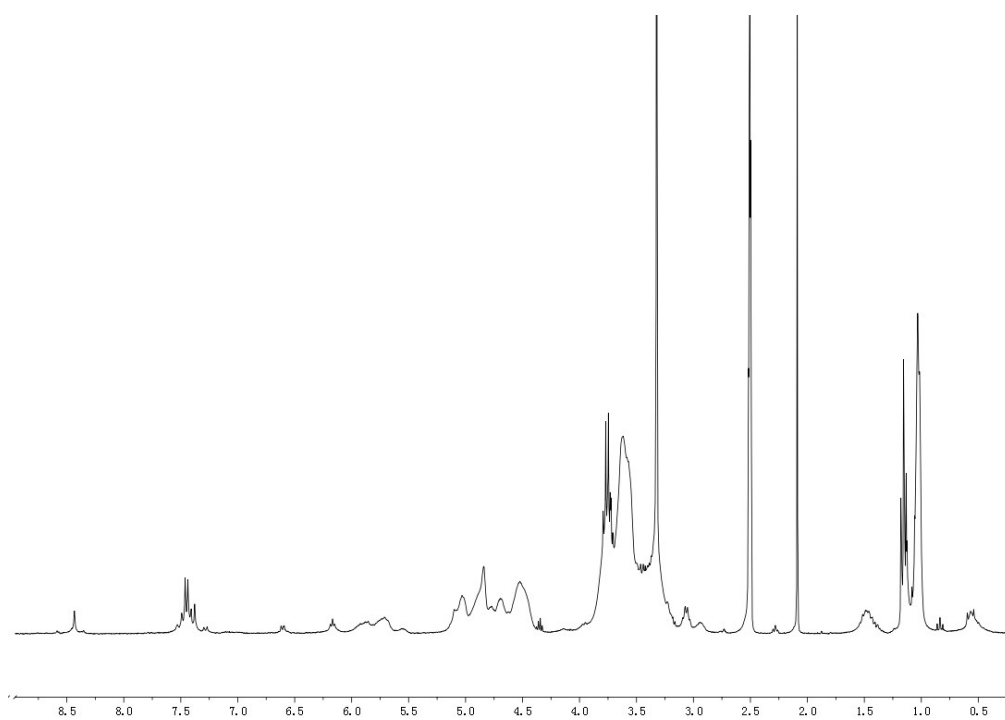


Figure S10. ^1H NMR spectrum of BpUcHpCD.

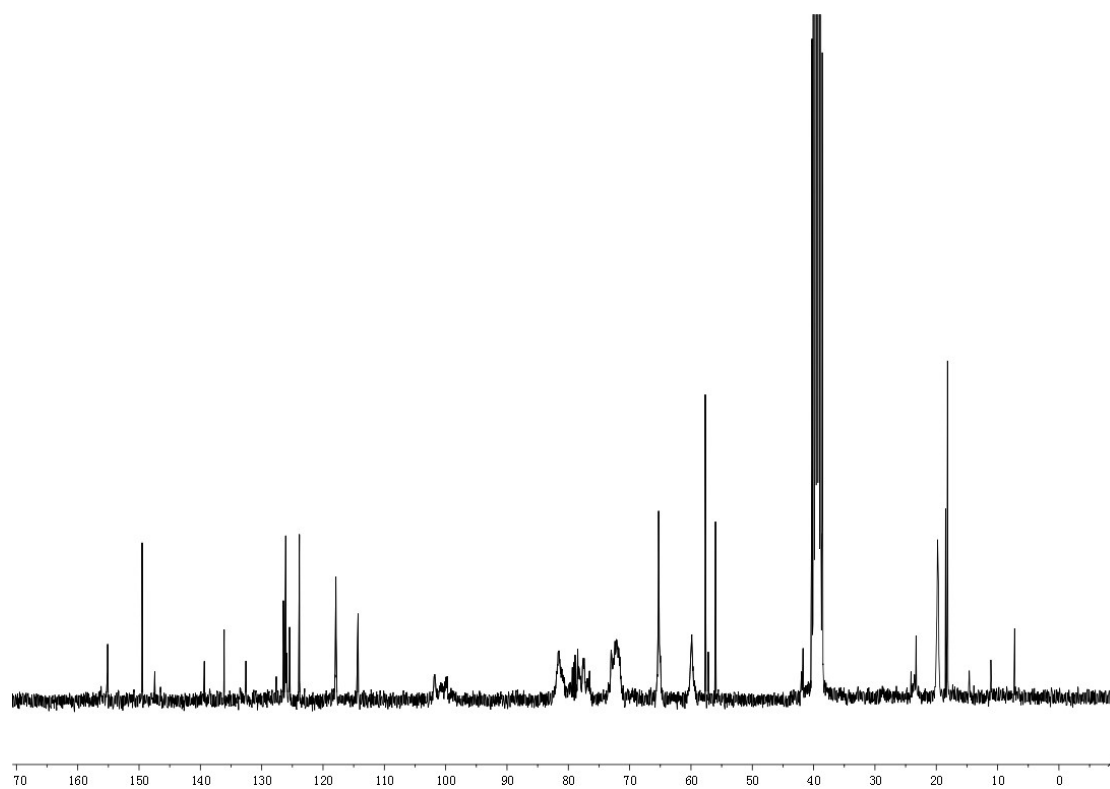


Figure S11. ^{13}C NMR spectrum of BpUcHpCD.

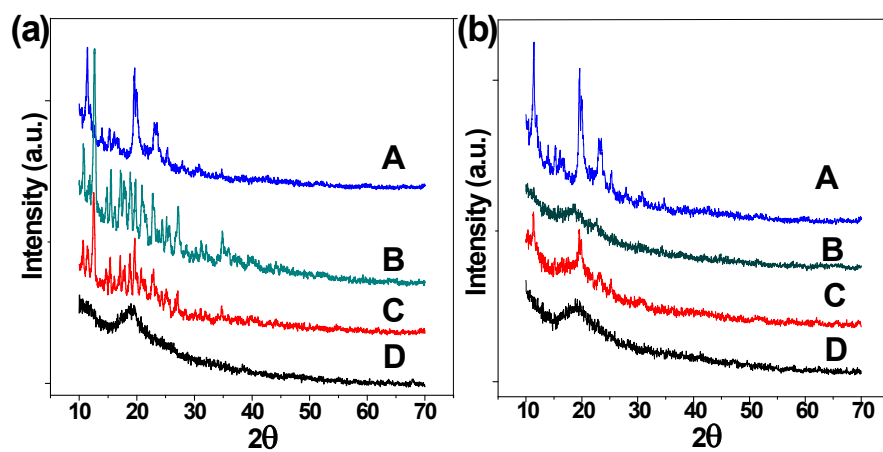


Figure S12. (a) XRD patterns of (A) BpU, (B) β -CD, (C) physical mixture of BpU and β -CD (1:2), (D) BpU \subset CD₂. (b) XRD patterns of (A) BpU, (B) Hp- β -CD, (C) physical mixture of BpU and Hp- β -CD (1:1), (D) BpU \subset HpCD.

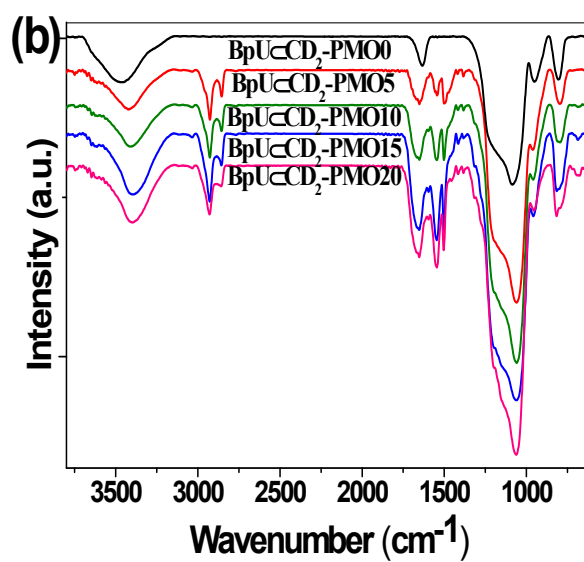
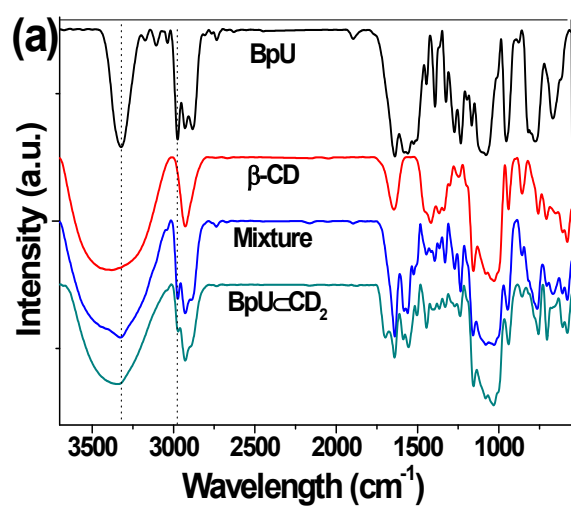


Figure S13. FT-IR spectra of (a) BpU, β -CD, physical mixture of BpU and β -CD (1:2), and BpU@CD₂ (b) BpU@CD₂-PMOs after extraction, from top being BpU@CD₂-PMO-X, X=0, 5, 10, 15, 20, respectively.

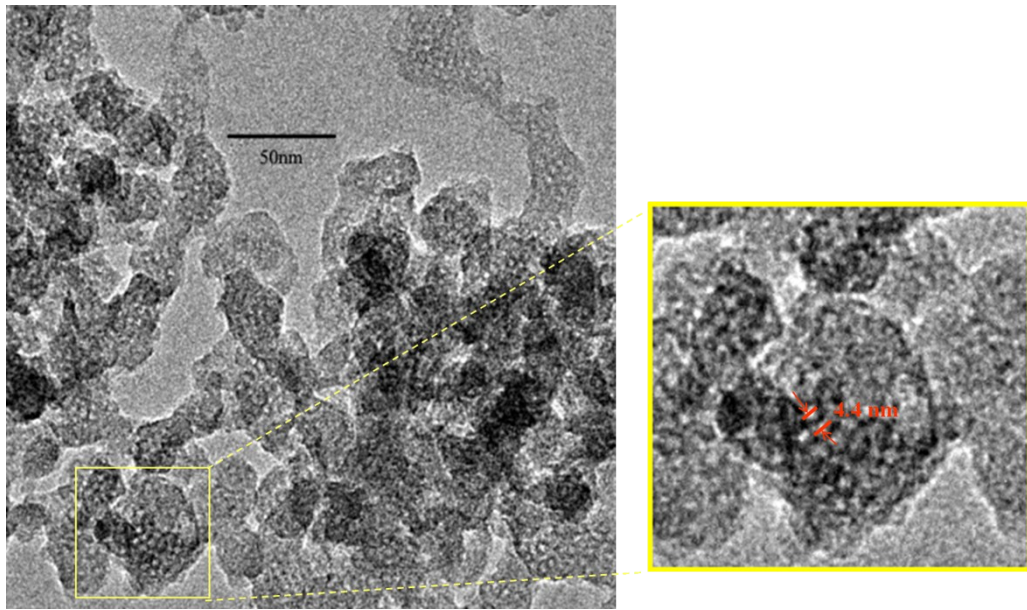


Figure S14. HRTEM images of BpUCD₂-PMO-5 after extraction of the template.

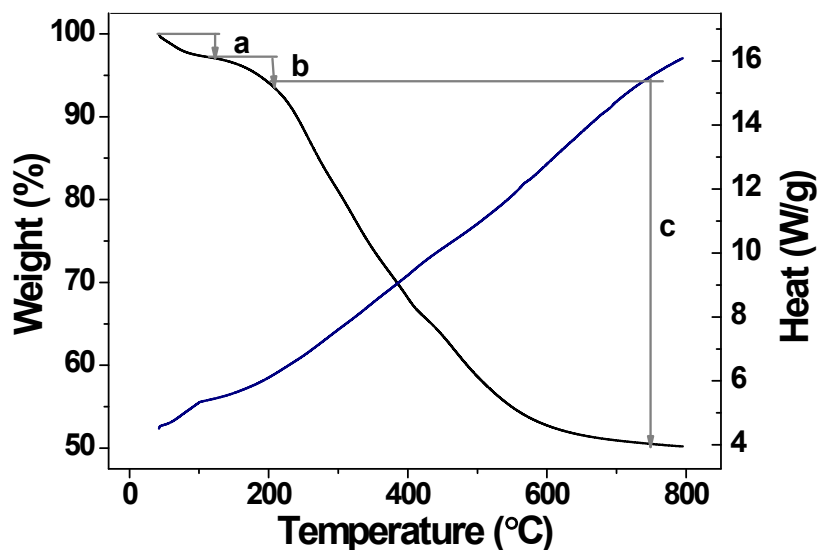


Figure S15. TGA / DSC of BpUCD₂-PMO-20

Thermogravimetric Analysis/Differential Scanning Calorimetry(TGA/DSC) was employed to study the thermal stability of the organic moieties of the hybrid materials. Figure S15 displays the TGA and DSC curves of the BpUCD₂-PMO-20 sample after removal of the template. About 2.7% of the mass loss is attributed to physisorbed water between 40 and 120°C. The mass decreases by 3.3% from 120 to 200°C due to elimination of crystalline water and the loss of water by the condensation of residual silanol and ethoxy groups. The mass continues to decrease gradually after 200°C to 50.6% at 800°C, which is ascribed to decomposition of the organic moieties. From the above analysis, the thermal stability of BpUCD₂-PMOs is maintained at 200°C completely.

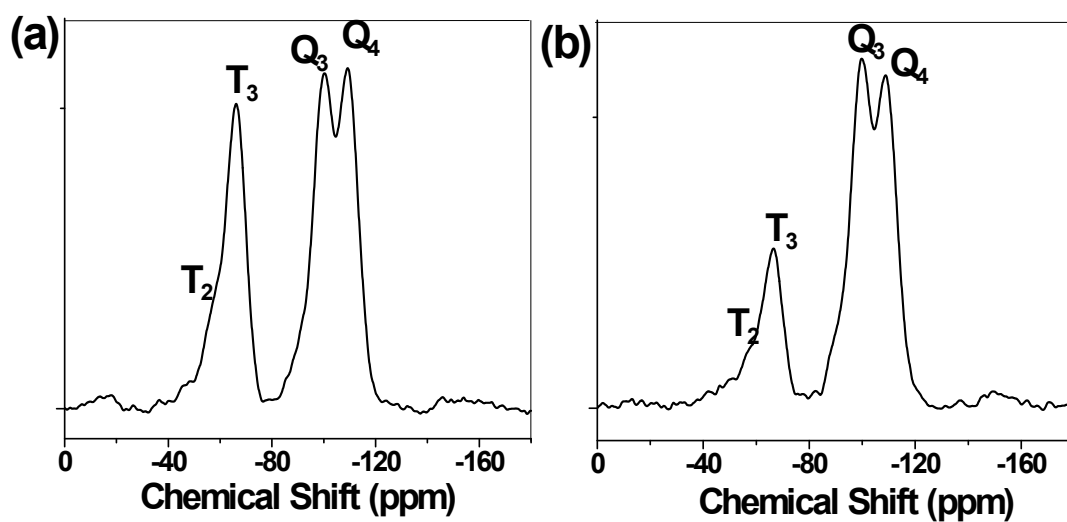


Figure S16. ^{29}Si MAS NMR spectra of BpU \subset CD $_2$ -PMO-20 (a) and BpU \subset HpCD-PMO-20 (b) after extraction of surfactant.

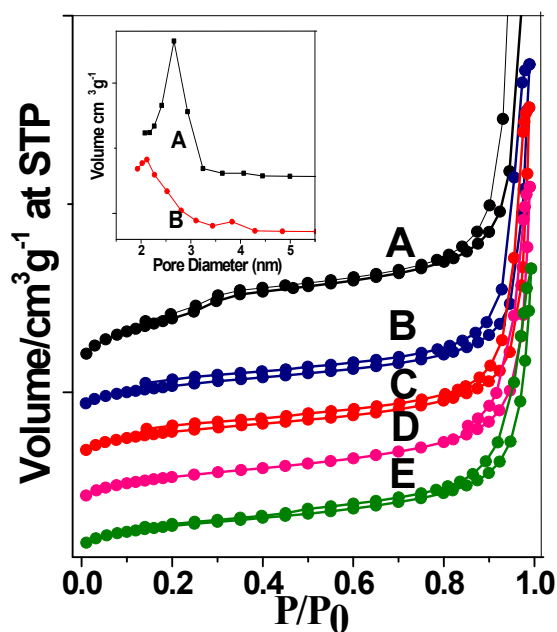


Figure S17. N₂ adsorption/desorption isotherms of BpUCD₂-PMO-X samples after extraction of surfactant. (A) X=0, (B) X=5, (C) X=10, (D) X=15, (E) X=20, respectively. Insert is the pore size distribution of BpUCD₂-PMO-0 and BpUCD₂-PMO-5.

Table S1. Surface properties of BpUCD₂-PMO-X samples

	BpUCD ₂ -PMO-0	BpUCD ₂ -PMO-5	BpUCD ₂ -PMO-10	BpUCD ₂ -PMO-15	BpUCD ₂ -PMO-20
$S_{BET}(m^2/g)$	606.4	237.3	242.0	256.4	239.0
$V_t(m^3/g)$	1.54	1.15	1.17	1.06	0.95
$D_{BJH}(nm)$	2.67	2.12	-	-	-

Nitrogen adsorption/desorption isotherms of the extracted BpUCD₂-PMO-X (X is from 0 to 20mol%) samples are shown in Figure S17. All the curves belong to type IV isotherms. The positions of the capillary condensation steps of the obtained isotherms move forward to low relative pressure (P/P_0) as the content of BpUCD₂ increases,

suggesting that the pore sizes of the obtained materials decrease gradually. Meanwhile, the pore size distribution calculated with the BJH method is centered at 2.12 nm for BpU \subset CD₂-PMO-5, which is smaller than that of BpU \subset CD₂-PMO-0 (2.67 nm). As indicated in Table S1, the surface areas, pore volumes, and pore sizes of BpU \subset CD₂-PMOs decrease when the rotaxane BpU \subset CD₂ amount is increased from 5 to 20 mol%, attributed to the incorporation of the rotaxane moieties into the mesostructure.

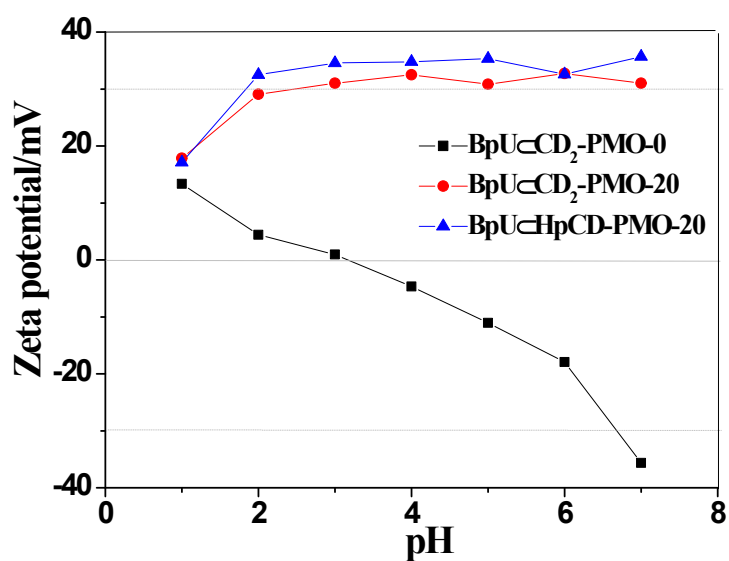


Figure S18. Zeta-potential of BpU \subset CD₂-PMO-0, BpU \subset CD₂-PMO-20 and BpU \subset HpCD-PMO-20 aqueous dispersions as a function of pH values

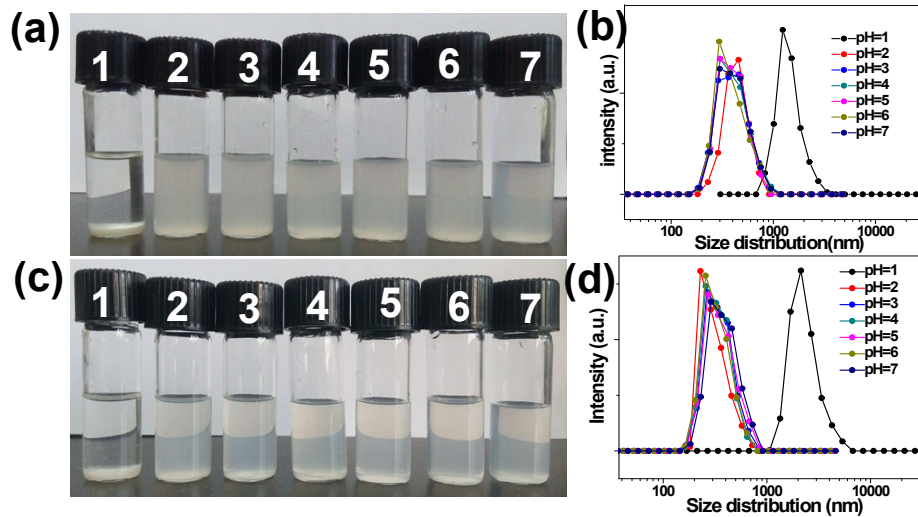


Figure S19. Dispersibility of (a) BpU \subset CD₂-PMO-20 and (c) BpU \subset HpCD-PMO-20 in water at different pH values; size distribution of (b) BpU \subset CD₂-PMO-20 and (d) BpU \subset HpCD-PMO-20 in water at different pH values.

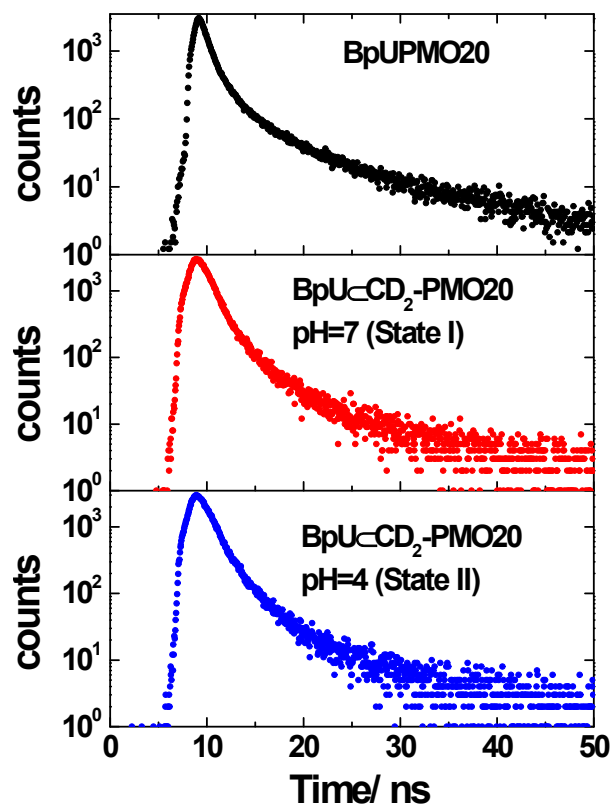


Figure S20. Fluorescence decay curves (ex 280 nm) of BpUPMO-20 without β -CD and BpU \subset CD₂-PMO-20 at pH= 7.0 (State I) and 4.0 (State II) , respectively.

Table S2. Fluorescence lifetimes of BpUPMO-20 and BpU \subset CD₂-PMO-20 in aqueous dispersion of different pH values (10⁻⁴ g/mL)

	τ_1/ns	τ_2/ns	τ_3/ns
BpUPMO-20 without β -CD	0.96	4.48	19.51
BpU \subset CD ₂ -PMO-20 (pH=7.0, State I)	1.21	4.25	34.18
BpU \subset CD ₂ -PMO-20 (pH=4.0, State II)	1.31	4.28	18.90

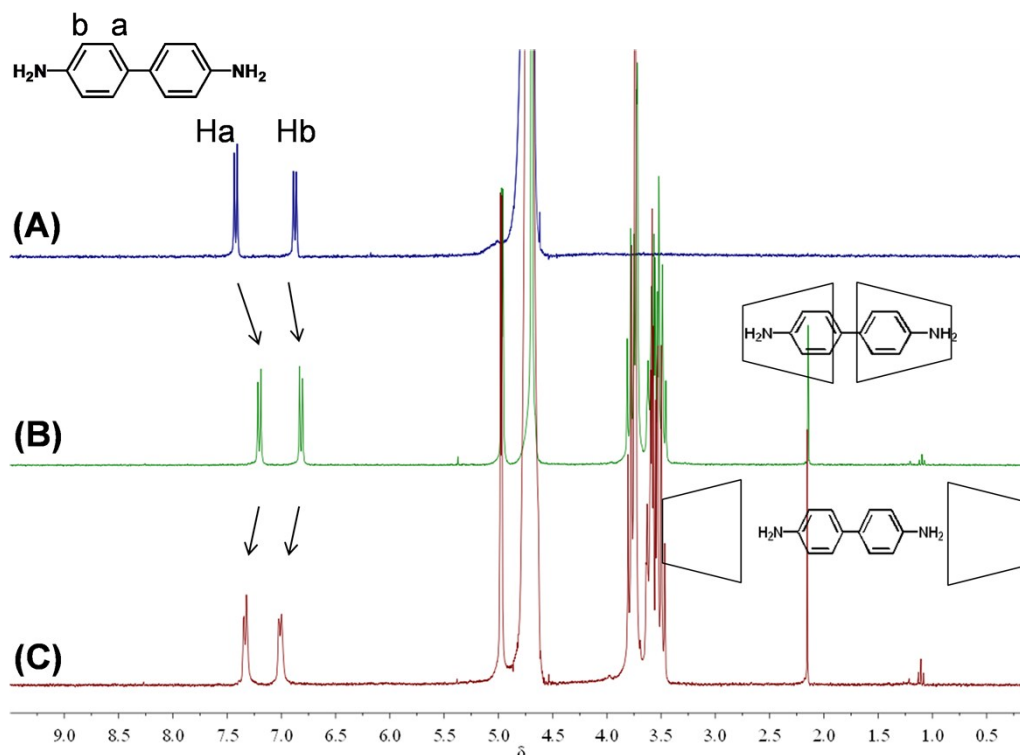


Figure S21. ¹H NMR spectra of benzidine (A), benzidine@CD₂ in neutral pH (B) and benzidine@CD₂ in acidic pH (C) in D₂O.

The movement of the β-CDs within the molecular shuttles was also monitored using ¹H NMR spectroscopy (Figure S21). H_a (7.41 ppm) and H_b (6.88 ppm) are the hydrogen atoms of the biphenyl rings in benzidine. Upfield shifts of approximately Δδ=0.21 ppm and Δδ=0.07 ppm are observed for H_a and H_b, respectively, compared with the spectra between the benzidine and benzidine@CD₂ (Figure S21A and B), suggesting that the aromatic rings of benzidine are inside the β-CD cavities. After the terminal amino groups are protonated with HCl solution (pH=3.0-4.0), the chemical shifts of H_a and H_b get right the original ones, showing that the benzidine molecules are detached from β-CD cavities (Figure S21A and C). The above information further confirms that the cyclodextrins are first located at the biphenyl group and then

transferred to the propyl chains by the acid stimuli, which is in accordance with the fluorescence analysis. The sudden change in the fluorescence emission position (~10 nm) occurs in the pH range of 4.0-5.0, which coincides with the acidic equilibrium constant (pKa=4.8) of the benzidine molecule, suggesting the positively charged benzidine unit dissociates from the β -CD cavity.

The preparation of benzidine \subset CD₂ ¹H NMR samples at different pH values is as follows: benzidine \subset CD₂ dissolved in D₂O and transferred 500 μ L to an NMR tube is regarded as neutral pH sample; acidic pH sample was obtained by adding 10 μ L of 0.01M DCl solution to 500 μ L benzidine \subset CD₂ aqueous solution.

Table S3. Energies and Assignments of the Observed Peaks in the *C* and *N K-Edge*

XANES Spectra.

	Resonance	Energy (eV)	Assignment
C K-edge	A	285.0	C $1s \rightarrow \pi^*_{C=C}$
	B	286.4	C $1s(C-N) \rightarrow \pi^*_{C=C}$
	C	288.2	σ^*_{C-H}
	D	289.5	C $1s \rightarrow \pi^*_{C=O}$
	E	292.5	σ^*_{C-C}
N K-edge	A	398.7	$\pi^*_{N=C}$
	B	399.9	π^*_{N-Ph}
	C	402.5	$\pi^*_{N-C=O}$
	D	406.4	σ^*

Only $1s \rightarrow \sigma^*$ transitions could be found in the β -CD molecules that contain sp³ carbon, therefore, the relative intensities of the $1s \rightarrow \sigma^*$ transitions (σ^*_{C-H} and σ^*_{C-C}) increase after the β -CDs are introduced into the PMO material.

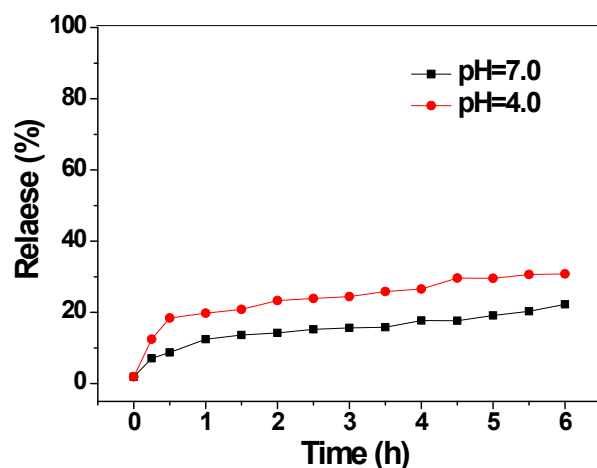


Figure 22. Release profiles of the Rh6G dye in the supernatant from the BpU⊂CD₂-PMO-0 material at pH 4.0 and 7.0.

The cargos release behaviors of BpU⊂CD₂-PMO-0 was shown in Figure S22. The results demonstrated that cargos release of BpU⊂CD₂-PMO-0 was also slightly pH dependent. This was because the zeta-potential of pure silica was slightly pH dependent due to the existence of silanols on the surface of BpU⊂CD₂-PMO-0. However, the released cargos amount of BpU⊂CD₂-PMO-0 could reach only 31% and 20% at pH=4 and 7 after 6 h, which indicated that the release amount of BpU⊂CD₂-PMO-0 between different pH was less significant. Consequently, the conversion between “OFF”/“ON” states was not significantly exhibited for the BpU⊂CD₂-PMO-0.